Politecnico
Milano 1863
SCUOLA DI INGEGNERIA INDUSTRIALE E DELL'INFORMAZIONE

Executive Summary of the Thesis

An electronic and crystallographic study of a ZnTPP thin film grown on Fe(001)-$p(1\times1)$O/Pd(001)

Laurea Magistrale in Physics Engineering - Ingegneria Fisica

Author: Giorgio Calandra

Supervisor: Dr. rer. nat. Isheta Majumdar

Co-Supervisor: Prof. Gianlorenzo Bussetti

Academic year: 2024-2025

1. Introduction

The fabrication of fully functional organic devices poses a significant challenge in preserving the chemical, physical and electronic properties of organic molecules when deposited on a substrate, such as a metallic one [1]. This challenge arises from the mutual interaction between the molecules and the substrate. In particular, the interaction that takes place at the inorganic/organic interface can modify the properties of both the substrate and the organic film (namely the *Surface Ligand Effect* (SLE)). The SLE plays a crucial role in the realisation of hybrid devices and has been exploited in various ways [2]. One of the most effective ways to passivate metallic substrates is the use of ultra-thin metal oxide (UTMO) films. A particularly relevant example is that of Fe(001)-$p(1\times1)$O (hereafter Fe-$p(1\times1)$O), where a single oxygen layer is incorporated into the four-fold symmetric "cavities" of the Fe(001) substrate surface [3] (see Fig.1(a)). The motivation for using UTMO stems from the possibility of exploiting the intrinsic properties of the Fe substrate, such as its conductivity and ferromagnetism, but at the same time introducing a decoupling layer between the metal substrate and the organic molecules to keep the properties of the molecules intact [4]. Among the various organic/inorganic interfaces, Zn tetra-phenyl-porphyrin (ZnTPP) on Fe-$p(1\times1)$O serves as a prototypical system to study the adhesion of organic films on UTMO layers and to study the processes involved in film growth. ZnTPP molecules consist of four pyrrole rings connected by methine bridges, forming a conjugated planar structure. At the skeleton border, four phenyl groups are linked to the main cavity of the molecule. The metal ion Zn^{2+} is located in the central ring and its presence alters the characteristic electronic properties of the molecule. The electronic and crystallographic features of a monolayer (ML) of ZnTPP deposited on a Fe-$p(1\times1)$O substrate have been extensively studied in an ultra-high vacuum (UHV) environment using organic molecular beam epitaxy (OMBE) [5, 6]. This molecular system displays long-range order, as confirmed by low-energy electron diffraction (LEED). In particular, the ZnTPP MLs are characterised by a (5×5) ordered reconstruction and well-recognisable electronic features in direct (PES) and inverse (IPES) photoemission spectroscopies. However, the correlation between the crystallographic and electronic properties of a ZnTPP ML on a Fe-$p(1\times1)$O substrate remains unclear. This work primarily investigates whether these properties are re-

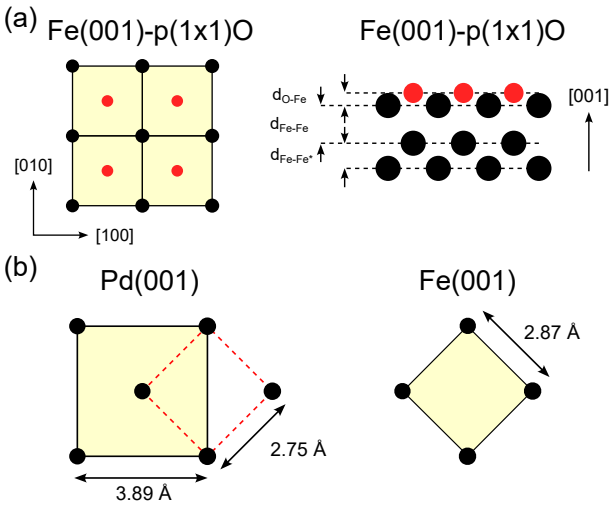

Figure 1: (a) Schematic of the Fe(001)-$p(1\times1)$O surface in its top and side views. The red circles represent the oxygen atoms that displace themselves in the hollow sites of the Fe lattice (black circles). In the side view relaxation makes the first interlayer distances vary. (b) Top views of the Pd(001) and Fe(001) surfaces.

tained when ZnTPPs are deposited on a lower quality Fe-$p(1\times1)$O surface. The lower crystalline quality is achieved by reducing the thickness of the Fe substrate, as thinner films often exhibit structural degradation [7]. Fe-$p(1\times1)$O is typically grown on a MgO(001) substrate with a thick Fe layer ($>$ 100 nm) [8]. However, for thinner Fe films ($\approx$ 5 nm), interdiffusion of oxygen from MgO to the surface can prevent proper growth. In this work, Pd(001) was chosen as the substrate to grow the Fe-$p(1\times1)$O surface. Depending on the crystal surface considered, the epitaxial growth of a Fe thin film on a Pd substrate can be either achieved or not. Although different metallic surfaces, e.g. Fe(110) on Pd(111), have been widely studied [9], most studies on Fe/Pd systems have been carried out with Pd(001) as substrate [10], as it is the easiest case to consider due to the relatively small lattice mismatch (see Fig.1(b)). However, Fe and Pd exhibit bulk miscibility, forming several stable ordered phases such as FePd and $FePd_3$ [11], making surface alloying highly probable. This phenomenon, called intermixing or interdiffusion, is strongly temperature-dependent. In particular, it has been observed that there is no alloying for Fe deposited on Pd at room temperature (RT) [12], whereas with increasing temperature the probability of intermixing increases, as demonstrated by J. H. Choi *et al.* [13]. In this work, a small amount of surface alloying was allowed. This can be removed by a long sputtering process and leaves room for the use of temperatures up to 350°C, resulting in better surface crystallinity.

In conclusion, this work aims to study the interconnection between electronic and crystallographic properties of an ML of ZnTPP deposited onto a thin layer of Fe-$p(1\times1)$O grown on Pd(001). Another aspect of this investigation is to study the influence of the metal-metal strains developed at the Pd/Fe interface on the assembling properties of porphyrins. For this purpose, the structural, chemical and electronic properties of 1 ML of ZnTPP deposited on Fe-$p(1\times1)$O grown on Pd(001) will be compared to those of 1 ML of ZnTPP deposited on Fe-$p(1\times1)$O grown on MgO(001) with predeposited 250 nm of Fe.

2. Materials and Methods

2.1. Fe(001)-$p(1\times1)$O on MgO(001)

To prepare the Fe-$p(1\times1)$O surface on MgO, we follow the well-established protocol by Bertacco *et al.* [8]. The sample preparation began in a UHV system (base pressure in high 10^{-11} Torr) with growing a 250 nm thick Fe(001) film on a clean MgO(001) single crystal substrate, by means of molecular beam epitaxy (MBE). At this thickness, the deposited Fe behaves as a bulk crystal [14]. We proceed by exposing the clean Fe(001) surface to 30 L (1 L = $1.0 \cdot 10^{-6}$ Torr $\times$ 1 s) of molecular oxygen (partial pressure of $2.0 \cdot 10^{-7}$ Torr, exposure time of 150 s) at 450 °C. Then, a higher temperature annealing at 700 °C follows for excess oxygen removal from the surface. In the following, such sample will be labelled as "*Ref.*". Once the Fe-$p(1\times1)$O surface has been prepared, we proceed by depositing the ZnTPP organic molecules in a dedicated vacuum chamber by means of Knudsen effusion cells. The ZnTPP film was deposited at an evaporation temperature of 270 °C thanks to dedicated temperature controllers which stabilize the crucible heating temperatures within 0.5 °C. The ZnTPP deposition rate was monitored by a quartz microbalance that registered a rate of about 0.9 Å/min. Since a complete mono-

layer (ML) coverage of ZnTPP corresponds to a thickness of approximately 3.9 Å [15], the deposition time can be precisely determined. Additionally, a 20 ML thick film of ZnTPP was grown on Fe-$p(1\times1)$O for comparison. This is because, at high coverage, i.e. > 4 ML [16], the spectra acquired on the thick film can be considered representative of the electronic properties of an isolated molecule and, therefore, any change in the spectroscopic features of the 1 ML film is usually interpreted in terms of molecule-substrate interaction. All the films were grown with the substrate kept at room temperature (RT).

2.2. Fe(001)-$p(1\times1)$O on Pd(001)

To prepare the Fe-$p(1\times1)$O surface on Pd, we replicate the procedure used by Eibl *et al.* in 2012 [17]. This starts with a series of sputtering/annealing cycles to clean the Pd surface. Then, it follows a 20 ML Fe deposition at RT for an overall thickness of about 5 nm. The clean Fe surface is exposed to oxygen at $3.7\cdot10^{-8}$ Torr at RT for 30 s (1L) and then annealing at 350 °C for 300 s completes the preparation. It is worth noting that the preparation parameters of oxygen quantity and temperature vary widely in the literature. After a preliminary analysis, in fact, we realized that the 1 L exposure was not enough to ensure a proper oxygen covering of the Fe surface. Therefore, thanks to a proper exposure analysis, the optimal exposure to get a proper Fe-$p(1\times1)$O surface was found to be 6 L ($3.0 \cdot 10^{-8}$ Torr for 200 s). Such a preparation protocol has to keep into account the strict limit in the temperature range due to the possible interdiffusion at the Fe/Pd interface. After the preparation of this substrate, we deposited 1 ML of ZnTPP with the same experimental parameters used for the reference sample.

2.3. Samples Characterisation

All samples were characterised by direct (PES) and inverse (IPES) photoemission spectroscopies and LEED. PES utilized non-monochromatic radiation from an ultra-violet (UV) He I ($h\nu$=21.2 eV) lamp for the UPS analysis and an X-ray Mg K_α ($h\nu$=1253.6 eV) anode source for the XPS analysis. All PES spectra have been subject to satellite peaks removal. Photoelectrons were collected in a 150 mm hemispherical electron analyzer [18], providing an overall energy resolution of 50 meV for the UPS and 100 meV for the detailed XPS spectra. A GaAs(001) photocathode, prepared according to standard procedures [19] used to achieve the Negative Electron Affinity (NEA) condition, was used for IPES. The operation mode was the isochromatic mode to detect 9.6 eV photons with a band-pass detector. The IPES energy resolution is about 600 meV. All the experiments reported here were achieved under negligible charging conditions during electron spectroscopy data acquisition. LEED was performed with a commercial apparatus equipped with a beam shutter. LEED images were taken at incident beam energies in the range of 55 and 100 eV before the spectroscopic characterizations, by exposing the sample to the electron beam for a few seconds.

3. Results and Discussion

3.1. Fe-$p(1\times1)$O/Pd Substrate

At first, we focus on the analysis of the substrate. The results of the first preparation [Fe-$p(1\times1)$O (1L)] are reported in Fig.2 together with the Eibl IPES spectrum (adapted with permission from Ref.[17]), the reference sample and the next preparation [Fe-$p(1\times1)$O (6L)]. Eventual differences in the shape and the position of the IPES peaks of the reference sample and the prepared sample with respect to the Eibl data may be due to differences in the IPES acquisition apparatus and resolution. It is evident from all data that the amount of oxygen in the 1 L sample is not enough to complete the Fe-$p(1\times1)$O preparation. Although in the IPES (see Fig.2(b)) the positions of the B1 and B2 peaks and the surface states S [20] are correct also for the 1 L case, it is evident that the relative height of the two peaks at 0.4 eV (B1) and 1.8 eV (B2) is not correct, i.e. the B2 peak should be 40% higher than B1 while for the 1 L the two are almost identical. Moreover, from the UPS spectrum in Fig.2(a), we note that the sharp peak at -4.3 eV, coming from oxygen valence states O 2p [21], for the 1 L sample is completely missing. Lastly, in the XPS (d) the O 1 s peak for the 1 L exposure is still far from the reference peak. The agreement with the reference sample improves as the oxygen exposure is increased up to 6 L. In the IPES spectrum, all

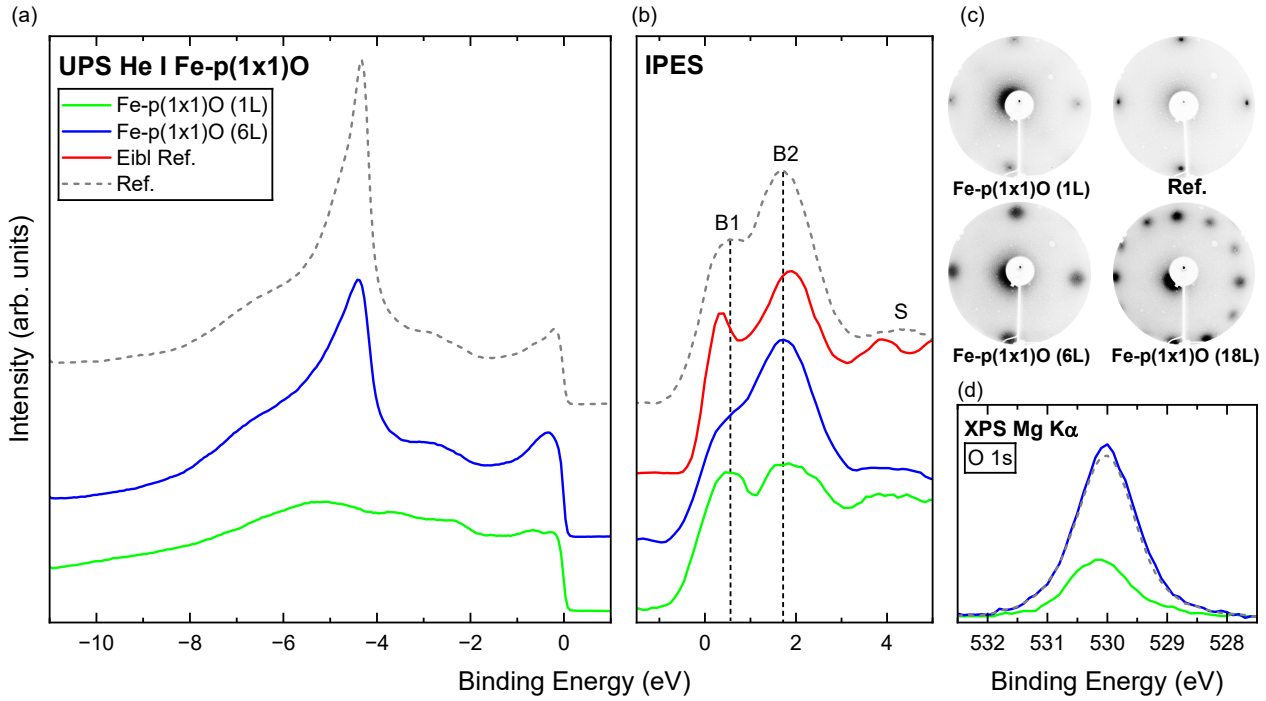

Figure 2: UPS (a), IPES (b) and XPS O 1s (d) spectra and LEED patterns (c) of the sample prepared with the Eibl protocol [Fe-$p(1\times1)$O (1L)], the one with the optimal exposure [Fe-$p(1\times1)$O (6L)], and the reference sample (Ref.). In the IPES spectrum (b), the samples are compared with the Eibl data (adapted with permission from [17]). The LEED patterns (c) were taken at an incident beam energy of 55 eV and include the overexposed pattern at 18 L.

the relevant features characterising a good Fe-$p(1\times1)$O, i.e. the two peaks B1 and B2 and the surface states S, are visible and in the correct positions. Nevertheless, we notice that the B1 peak in the 6 L is less marked than the two reference cases, although the relative height of B2 with respect to B1 is almost the same for the two samples and approximately equal to 1.5. We also notice a slight broadening of the B2 peak for the 6 L sample with respect to the reference one. The broadening is also observed in the O 2p peak at -4.3 eV in the UPS spectrum, where the greater sharpness of the reference sample's peak is more evident. However, this represents a great improvement to the 1 L sample since the XPS shows an almost perfect amount of oxygen for the 6 L case (see Fig.2(d)). However, the LEED pattern of the 6 L sample exhibits quite broad spots forming a (1×1) superstructure. The increased dimension of the spots and their dispersed nature compared with that of the reference sample denotes a worsening in the crystalline quality of the Fe-$p(1\times1)$O surface. Lastly, we observe that increasing the oxygen exposure up to 18 L gives rise to a LEED pattern (see Fig.2(c)) of a superstructure called the *Hex* phase [22].

3.2. ZnTPP on Fe-$p(1\times1)$O/Pd

Given the analysis of the substrate, it is evident that the exposure to 6 L of oxygen gives the best substrate for the deposition of the organic film. The UPS and IPES analyses of the ZnTPP film are shown in Fig. 3(a)-(b). Each peak was assigned to a ZnTPP molecular component based on the theoretical study by Rangan *et al.* [23]. The UPS spectrum (a) of the 6 L sample is in almost perfect agreement with that of the reference sample with the single layer of porphyrins. Both the 1 ML ZnTPP spectra are shifted towards lower binding energies by about 0.4 eV, and the molecular features are evident, especially those associated with the phenyls groups (Ph). The HOMO (TPR1) feature at -1.5 eV in the 6 L sample is less pronounced compared to the reference. This quenching may result from either a stronger molecule-substrate interaction or non-uniform molecular film growth. Nevertheless, as already proven [24], the evidence of the ring contribution, i.e. HOMO (TPR1) and

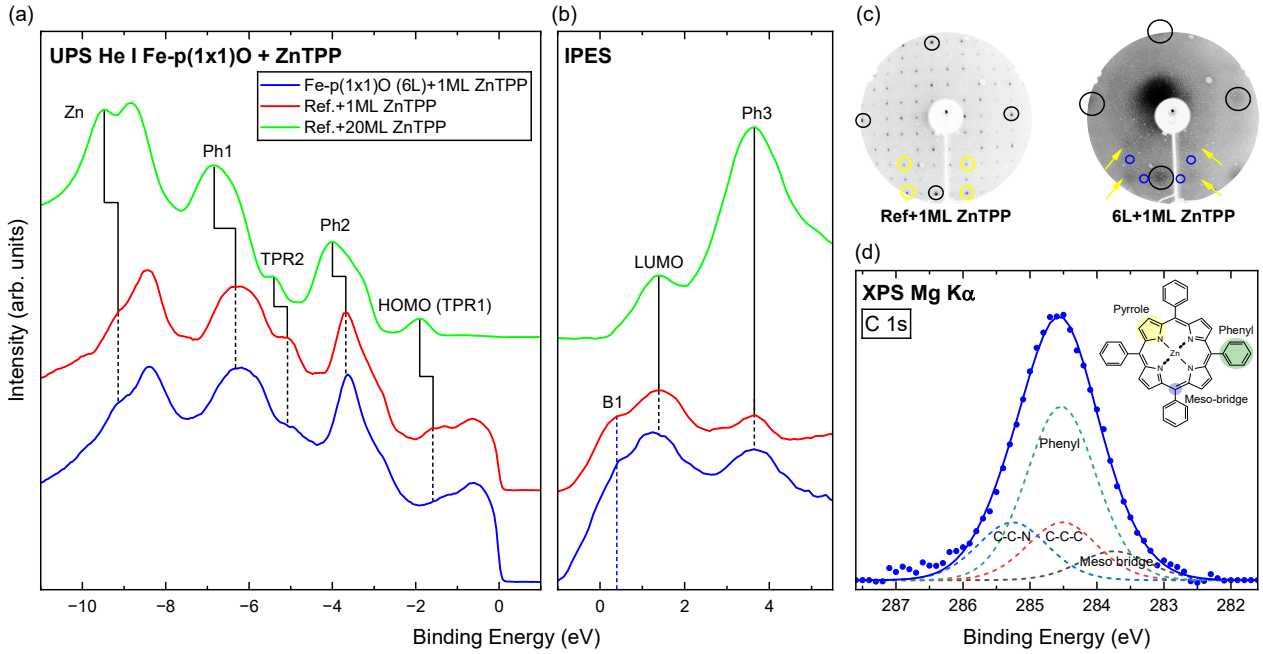

Figure 3: UPS (a), IPES (b) and XPS C 1s (d) spectra and LEED patterns (c) of the optimally exposed sample [Fe-$p(1\times1)$O (6L)] and of the reference sample (Ref.) with 1 ML of ZnTPP deposited on them. In the UPS (a) and IPES (b) spectra the 20 ML of ZnTPP coverage is reported for comparison, too. In the LEED pattern (c) for the 6 L sample, the arrows show those spots that could indicate a faint (5×5) reconstruction, the black circles indicate the underlying (1×1) reconstruction of the Fe-$p(1\times1)$O substrate and the blue circles indicate the missing spots of the faint (5×5) reconstruction. In the XPS peak (d) the four contributions for the carbon feature used for the deconvolution together with the experimental data (blue dots) and the fit envelope (solid blue line) are reported.

TPR2, in the UPS data is a fingerprint of a good decoupling between the buried substrate and the molecules. Moreover, the stoichiometry analysis performed, such as the C 1s peak deconvolution (d), ensures that porphyrins are preserved during the sublimation and their growth on the iron oxide substrate. The IPES spectrum (b) does not present significant variations with respect to the reference case, too. In the IPES (b), we notice that a residual trace of the B1 peak (0.4 eV) is still visible in the spectrum of the single layer of ZnTPP. Furthermore, the relative height of the LUMO and the Ph3 peaks is almost the same for the two 1 ML ZnTPP samples: 1.2 and 1.3 for the 6 L and the reference sample, respectively. LEED patterns (c) show that the crystallographic order of the molecular layer for the 6 L sample is almost completely lost and, in any case, is different from that of the reference sample, where an almost perfect (5×5) superstructure is observed. Nevertheless, we can discern a hint of such a reconstruction. In the image, some spots belonging to a possible (5×5) reconstruction are visible (see the yellow arrows), although very faintly. In particular, in the (5×5) superstructure of the reference case, we observe the spots in these same positions being brighter than others (see yellow circles), with a well-defined symmetry, i.e. brighter and lighter spots appear in an alternated manner. This order of the diffraction spots is maintained in the 6 L sample, in which we only observe those spots that appear brighter in the proper (5×5) superstructure on the reference sample. These are separated by missing spots (see blue circles) that correspond to the lighter ones in the proper (5×5). In conclusion, the 6 L sample does not exhibit a proper (5×5) reconstruction, showing a reduced, if not completely missing, crystallographic ordering of the molecular overlayer.

4. Conclusions

This study provides a comprehensive investigation into the electronic and crystallographic properties of a ZnTPP monolayer deposited on Fe-$p(1\times1)$O/Pd(001). The results highlight

a striking decoupling between the molecular electronic states and the crystallographic order of the ZnTPP film. While the electronic structure, as probed by PES and IPES, remains largely unaltered compared to the reference system (ZnTPP/Fe-$p(1\times1)$O/MgO), the long-range (5×5) molecular ordering observed in the latter is absent when the Fe(001)-$p(1\times1)$O layer is grown on Pd(001). This suggests that the metal-metal strain at the Pd/Fe interface disrupts the molecular self-assembly while preserving the electronic properties of the organic layer.

5. Acknowledgements

I want to thank all the people at the VESI lab for their support and for giving me the opportunity to write this thesis.

References

[1] N. Ueno, N. Koch, and A. T. S. Wee. *The Molecule–Metal Interface*. John Wiley & Sons, L., 2013. Chap. 1, pp. 1–14.

[2] G. Bussetti et al. *Advanced Functional Materials* 24.7 (2014), pp. 958–963.

[3] A. Picone et al. *Phys. Rev. B* 83 (23 June 2011), p. 235402.

[4] Q. Fu et al. *Science* 328.5982 (2010), pp. 1141–1144.

[5] G. Bussetti et al. *Applied Surface Science* 390 (2016), pp. 856–862.

[6] I. Majumdar et al. *Applied Surface Science* 636 (2023), p. 157807.

[7] D. T. Yimam and B. J. Kooi. *ACS Applied Materials & Interfaces* 14.11 (2022), pp. 13593–13600.

[8] R. Bertacco, S. De Rossi, and F. Ciccacci. *Journal of Vacuum Science & Technology A* 16.4 (July 1998), pp. 2277–2280.

[9] L. R. Merte et al. *The Journal of Physical Chemistry C* 115.5 (2011), pp. 2089–2099.

[10] X. F. Jin et al. *Phys. Rev. B* 60 (16 Oct. 1999), pp. 11809–11812.

[11] J. J. M. Franse and R. Gersdorf. 1st ed. Landolt-Börnstein: Numerical Data and Functional Relationships in Science and Technology - New Series. Springer Berlin, H., 1997.

[12] H. L. Meyerheim, R. Popescu, and J. Kirschner. *Phys. Rev. B* 73 (24 June 2006), p. 245432.

[13] J.-H. Choi et al. *Surface Science* 495.1 (2001), pp. 173–184.

[14] A. Calloni et al. *Applied Surface Science* 505 (2020), p. 144213.

[15] M. S. Jagadeesh et al. *Applied Physics Letters* 115.8 (Aug. 2019), p. 082404.

[16] G. Bussetti et al. *Beilstein Journal of Nanotechnology* 7 (2016), pp. 1527–1531.

[17] C. Eibl, A. B. Schmidt, and M. Donath. *Phys. Rev. B* 86 (16 Oct. 2012), p. 161414.

[18] G. Berti et al. *Review of Scientific Instruments* 85 (July 2014), pp. 073901–073901.

[19] F. Ciccacci and G. Chiaia. *Journal of Vacuum Science & Technology A: Vacuum, Surfaces, and Films* 9.6 (1991), pp. 2991–2995.

[20] S. De Rossi, F. Ciccacci, and S. Crampin. *Phys. Rev. Lett.* 77 (5 July 1996), pp. 908–911.

[21] A. Clarke et al. *Phys. Rev. B* 41 (14 May 1990), pp. 9659–9667.

[22] D. Kuhness et al. *Surface Science* 645 (2016), pp. 13–22.

[23] S. Rangan et al. *The Journal of Physical Chemistry C* 114.2 (2010), pp. 1139–1147.

[24] G. Bussetti et al. *Applied Surface Science* 514 (2020), p. 145891.